

## Deep Seismic Imaging and Velocity Estimation in Ionian Sea

E. Kokinou<sup>1</sup>, A. Vafidis<sup>1</sup>, M. Loucogiannakis<sup>2</sup>, I. Louis<sup>3</sup>

<sup>1</sup> Applied Geophysics Lab. Dep. of Mineral Resource Eng. Technical Univ. of Crete,  
Chania, Greece 73100.

[ekokinou@mred.tuc.gr](mailto:ekokinou@mred.tuc.gr) ; [vafidis@mred.tuc.gr](mailto:vafidis@mred.tuc.gr)

<sup>2</sup> Hellenic Petroleum (Exploration and Exploitation of Hydrocarbons Division),  
Maroussi, Athens, Greece.

<sup>3</sup> Dep. Of Geophysics, University of Athens, Athens.

[jlouis@geol.uoa.gr](mailto:jlouis@geol.uoa.gr)

Corresponding author. Tel.: +32-8210-37643; Fax: +32-8210-37603

---

**Abstract:** *The seismic data from a deep seismic profiling (DSP) survey in Ionian Sea which crosses the western border of the Hellenic arc have been reprocessed and interpreted. The processing flow includes multiple elimination techniques such as wave equation multiple rejection and adaptive deconvolution.*

*Special processing helped in delineating complex structures in the Pre-Apulian and Ionian zones. Surface consistent deconvolution, Kirchhoff migration and attributes proved useful in imaging deeper horizons, in the area near the Zakynthos and Kefallinia islands where Mouna fault constructional structure and Kefallinia diapir are present. In this area the seismic section indicates that the Plio-Quaternary sediments are distorted by diapiric movements of high velocity Triassic evaporates, namely the Kefallinia Diapir. Also the eastern boundary of Ionian zone is observed under the Mouna anticline.*

*The velocity model along the seismic line ION-7, which crosses the Ionian basin is also presented. The Moho discontinuity is estimated in the western part of the seismic section, while Moho reflections are absent in the eastern part.*

---

**Keywords:** *Ionian basin, Deep reflection profiling, Velocity model, Stacked section, Migrated section.*

### INTRODUCTION

Deep Seismic Profiling (DSP) is useful in obtaining information about the structure of the crust and the upper mantle (Klemperer et al., 1985). Deep reflections at near – normal incidence were reported in the context of COCORP (Consortium for Continental Reflection Profiling, USA, Matthews and Smith, 1987). In the First International Symposium held in Cornell (1984) fifty – nine papers have been presented (Barazangi and Brown, 1986).

In seismic images from deep structures two reflection patterns have been observed. The first is characterized by the abundance of seismic reflections in the lower crust and mantle, while in the second the reflections are sparse. The reflection from the Moho discontinuity in the former pattern can not be easily distinguished.

A great progress in the crust and upper mantle probing using the seismic reflection method maintained has been realized by research groups and/or national

research programs, such as BIRPS (British Institutions Reflection Profiling Syndicate), ECORS (Etude de la croûte Continentale et Océanique par Réflexion et Réfraction Sismiques, France), DECORP (Deutsches Kontinentales Reflexionsseismisches Program, Germany), ACORP (Australian Continental Reflection Profiling), ADCOH (Appalachian Ultradeep Core Hole), CALCRUST (California consortium for Crustal Studies) and LITHOPROBE (Canadian program for the study of the continental lithosphere).

Offshore the British Islands, in the continental margin NW of England, a DSP survey indicated that the Moho discontinuity appears at 27 km in the continental crust and at 15 km in the oceanic crust. Reflections from fault zones in the upper crust become progressively subhorizontal in the lower crust. Although Moho discontinuity is considered as a stable interface between crust and mantle, it was suggested that it is a relatively new structure originating from extension processes.

Wide angle seismic reflection studies in the Rhine graben (Damotte et al., 1987) illustrated that a simple velocity model can be utilized for the crust consisting of three layers. The deeper crustal layer exhibits a velocity of about 6.9 Km/s and maximum depth of 25 Km. In the Black Forest (Germany), similar studies indicate that the Moho appears as a flat horizontal first order discontinuity at a relatively shallow depth of 25 – 27 Km (KTB – Research Group Black Forest, 1987).

According to deep reflection seismic measurements carried out in 1992 on a profile south of Rechnitz, Burgenland in Austria, the Moho discontinuity is defined at a depth of about 30 Km (Weber et al., 1996). The main result concerning the deep structure from seismic studies in the southwestern part of the Transcarpathian Depression is the (Vejmelek and Tomek, 1989) relatively small crustal thickness 26 Km which is a consequence of extension and associated basin subsidence. In the Tyrrhenian Sea (Italy), the crust thickness ranges between 15 and 25 Km (Giese and Morelli, 1973). Finetti and Morelli (1973) determined a crust (possibly oceanic)

thickness of 12 Km in the Tyrrhenian Bathyal Plain.

In the context of refraction seismics on two cruises of the research ship “Meteor”, Weigel (1974) estimated the Moho at a depth of about 46 Km under the western coast of Peloponnesus, while the transition zone to the upper mantle rises to 18 Km under the western part of the Mediterranean Ridge and the Ionian Abyssal Plain. Makris (1975) proposed a 2 – D crustal model between the Malta Shelf and Turkey based on gravity, magnetic and deep seismic soundings. The Moho depth is estimated at about 38 – 40 Km under the Malta Shelf, reduces to 20 Km in the Ionian Abyssal Plain, increases at more than 40 Km under Peloponnesus and ranges between 35 – 45 Km in Aegean Sea and Turkey. A later study by Makris et al. (1986) based on OBS data estimated the Moho depth in the Ionian Abyssal Plain at about 11 Km. Moretti and Royden (1988) analyzed gravity and deflection data and proposed the doubly subducted continental lithosphere model based on gravity and deflection data from the Adriatic and Ionian seas.

The Ionian basin comprises a deep sedimentary basin including Mesozoic to Tertiary sequences (Dercourt et al., 1986). The Ionian abyssal plain possibly floored of oceanic crust, which is subducted beneath the Hellenic and Calabrian Arcs (Weigel, 1974; Makris et al., 1986; Underhill, 1989). The high Bouguer anomalies at the center of the Ionian abyssal plain (+300 mGal, Morelli et al., 1975) are consistent with the thinned crust found by Hinz (1974) in the southern Ionian abyssal plain. An active dextral wrench zone, the Kefallinia transform fault, separates the oceanic crust from the end - wedge of the Mediterranean Ridge (Finetti, 1982). A deep seismic experiment was carried out in Ionian Sea in order to image the structure of the crust in a geologically complex area. This seismic line crosses the Ionian Abyssal plain and the Ionian basin.

In this paper a short description of the seismic experiment is followed by the seismic data processing steps. Special data processing methods like surface consistent deconvolution, Kirchoff migration and

attribute analysis are briefly presented. The results from the application of these methods are finally discussed. The velocity model is also described and utilized in the interpretation of the seismic section.

### THE SEISMIC REFLECTION EXPERIMENT

The Deep Seismic Profiling (DSP) in Ionian Sea was carried out in 1992 within the framework of the STREAMERS Project supported by the European Union (Joule Project STREAMERS), in order to obtain information about the structure of the crust in the Ionian basin. Seven seismic lines (Fig. 1) of total length 700 Km were scanned in the central Mediterranean Sea. One of these lines namely ION – 7 crosses the deep Ionian basin to the Patras Gulf.

The seismic data were recorded by Geco-Prakla's M/V Bin Hai 511 which towed a 36 – airgun tuned array with a capacity of 7118 inch<sup>3</sup> (about 120 l). A 180 - channel streamer array produced a 30-fold normal incidence reflection profile. The shot interval was 75 m, the

receiver interval 25 m, the minimum offset 180 m, the sampling interval 4 ms, the number of shots 2385, the recording length 22 s and the common midpoint sampling 12.5 m.

The seismic sections for the lines ION – 1 to ION – 6 show a layered band of reflectors with strong amplitudes at the deeper crust (Nicolich et al., 1994). These reflectors are attributed to a 3.5 – 4 Km thick laminated lower crust or crust – mantle transition. Hirn et al. (1996) interpreted the seismic section ION – 7 in combination with wide angle seismic data from 12 land stations in the surrounding islands and the mainland around Patras gulf. A major reflector at a depth of about 13 Km is attributed to the lower limit of western Hellenides. On the seismic section, disruptions of the Mesozoic sequence suggest a more westerly position for the Ionian thrust than previously considered. In the eastern portion of the seismic section diapiric movements of Triassic evaporites are observed, while the reflector at a depth of about 6 – 7 Km is interpreted as the “decoulement surface” of the folded belt within the Triassic evaporites (Kamberis et al., 1996).

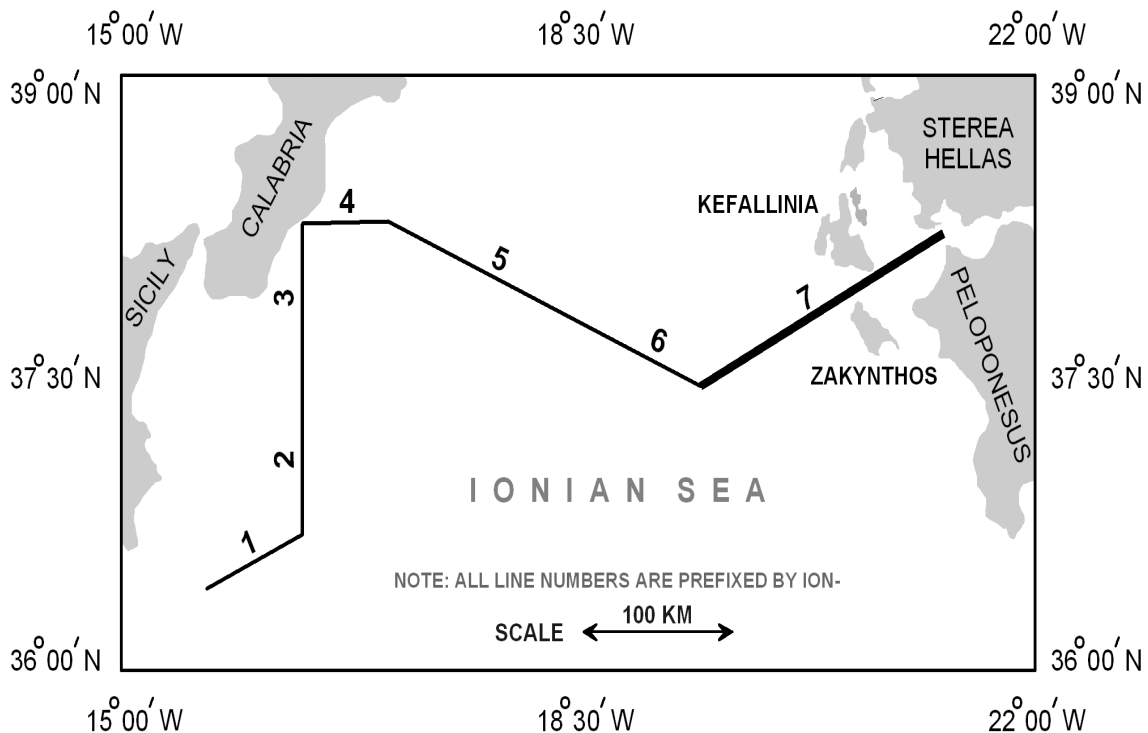


FIG. 1: Map of STREAMERS – lines.

## SEISMIC DATA PROCESSING FLOW

Seismic data processing aims at uncovering primary reflections by suppressing noise of various types, reducing the seismic data volume to the plane of zero – offset seismic section and finally increasing the signal to noise ratio and the lateral resolution. The data processing steps for seismic line ION – 7 are presented in Table (1). The first two steps are resampling from 4 ms to 8 ms and geometry verification. Prestacking steps include multiple attenuation and seismic velocity analysis.

The reflection data along the seismic line ION-7 exhibit strong sea-bottom and internal multiples from deep and shallow water-bottom, lateral reflections and coherent noise. The above mentioned seismic events imposed difficulties in recognizing the reflections, especially from deeper horizons. Shot records were processed using wave equation multiple rejection (Wiggins, 1988) and adaptive deconvolution (Griffiths et al., 1978) in order to attenuate the sea – floor multiple reflections and the non periodic internal multiples (peg – leg and ghosts) (Kokinou and Vafidis, 2002). On the stacked section resulting from the demultiple procedure, the seafloor and internal multiples are adequately suppressed (Fig. 2 a, b).

Special emphasis was given to seismic velocity analysis by using the semblance method. Portions of the velocity model are described in the following chapter. Spherical divergence correction was applied to compensate for loss of amplitudes using the RMS – velocities. A top mute was applied to remove events at times earlier than the sea floor reflection.

Trace mixing and equalization (2D Promax Ref.) have been applied after stacking. The weighted median mix algorithm sorts nine samples within the trace mix window, along with their weights. When the weights of the ordered sequence total greater than one – half the sum of the mix weights, this point is selected as the weighted median, and is passed as the mixed sample value. Trace equalization computes and applies a trace to trace amplitude balancing function. The

stacked sections including the interpretation are discussed in the following chapter.

**Table 1** Prestack and poststack processing Sequences

PROCESSING SEQUENCE OF LINE ION - 7
1. Data editing
2. Resampling: 8 ms
3. Geometry
4. Wave equation multiple rejection
5. Autocorrelation
6. Deconvolution
7. Sorting: 12.5 m interval, CDP gathers
8. Automatic gain control: 1000 ms
9. Velocity analysis
10. Geometrical spreading correction
11. Top mute
12. NMO - Stacking
13. F – K filters (Fan – filters): 1500 – 5500 m/s, 5 – 18 Hz
14. Surface consistent deconvolution
15. Kirchhoff Migration
16. Trace mix: 0 –22 s, 9 trace mix
17. Trace equalization
18. Instantaneous attributes and Hilbert transform

## IONIAN SEA VELOCITY MODEL

Velocity analysis has been performed on selected CDP gathers. The spacing of successive CDP gathers is 125-187.5 m for moderately dipping sea bottom and 375-500 m for flat sea bottom. From the CDP gather, the Normal moveout (NMO) – corrected CDP gather and the velocity spectrum the RMS-velocities are picked (Fig. 3). In this chapter we describe in detail the velocity model along the ION-7. We also use it in the interpretation of the seismic section. The velocity model is divided in four portions namely the Ionian Abyssal Plain (IoAP), the Mediterranean Ridge, the Hellenic Arc and the eastern portion of ION-7.

On the velocity model and the stacked section (Fig. 4) at the western portion of ION-7 the Ionian Abyssal Plain is observed with almost flat sea-bottom. The average velocity in the shallow layers

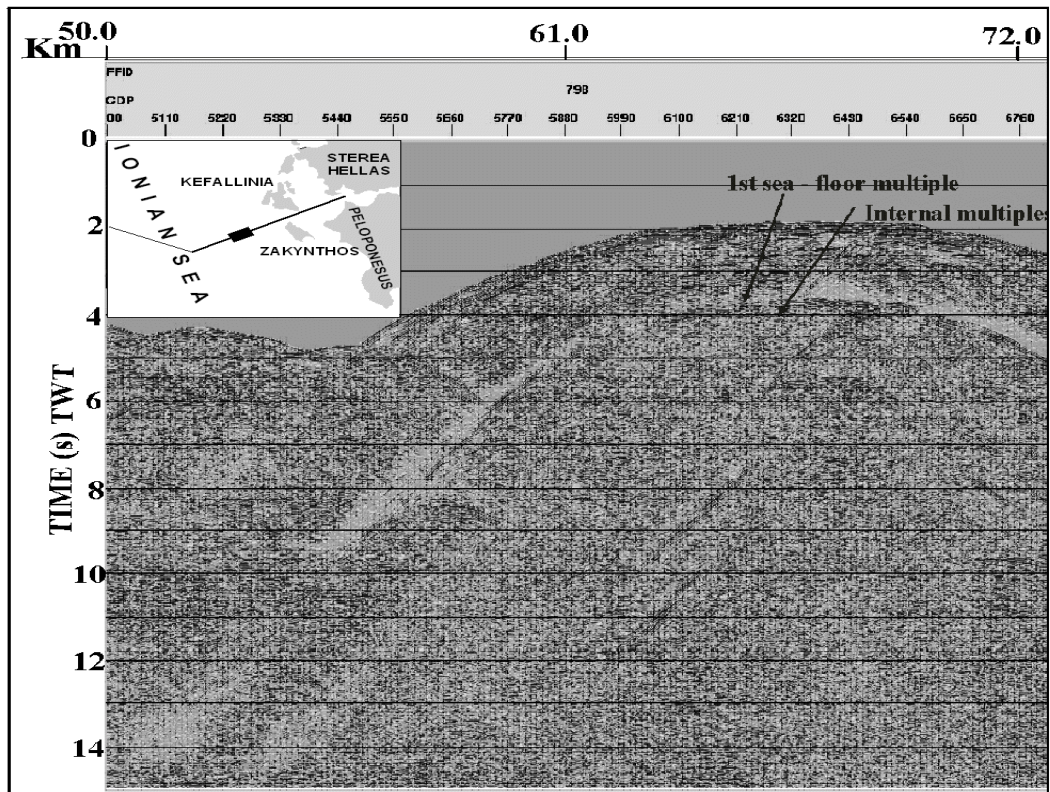


FIG. 2 (a): Stacked section before the application of the prestack demultiple procedure. The sea floor multiple and internal multiples have been removed.

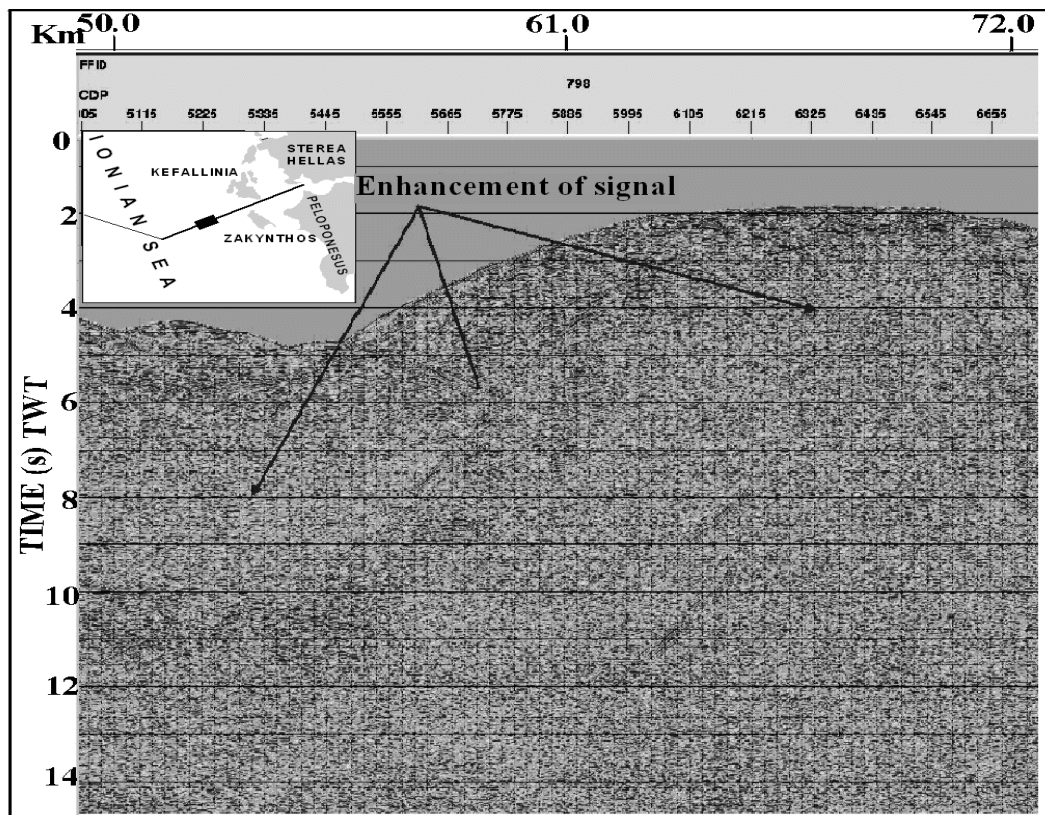


FIG. 2 (b): Stacked section after the application of the demultiple procedure. The sea floor multiple and internal multiples have been removed.

(4.25 s to 4.7 s TWT) attributed to Messinian, Pliocene – Quaternary sediments (Mess, P – Q) is 4 Km/s. A low velocity layer (3.5 Km/s) is detected between 4.6 and 5.5 s TWT, which is attributed to Mesozoic, Pre – Messinian (Me, Pre – Mess) sediments (Fig. 4b). The velocity in the underlying layers ranges from 5 to 7.5 Km/s. A deeper layer exhibits high seismic velocity (7.5 – 9 Km/s) and is attributed to the upper mantle. Although velocity analysis at the deeper portion of the seismic section becomes less accurate, the existence of this high velocity zone suggests that the Moho discontinuity is located at depth of 12 Km.

East of the Abyssal Plain, there is a broad bathymetric high (Mediterranean Ridge) which is separated from the IoAP by the Kefallinia fault (KEF, Fig. 5).

This fault according to seismological evidence is characterized by strike – slip motion combined with a thrust component (Louvari et al., 1999), while geological information further support the existence of right - lateral strike - slip faults in the western part of Lefkada Island (Underhill, 1989, IGME, Seismotectonic map). Below the Mediterranean Ridge, the seismic velocity of the Plio-Quaternary (P- Q) sequence ranges from 2.5 to 3 km/s (Fig. 5a). In this layer sporadic high velocity zones (4.5 – 5 Km/s) are present which possibly correspond to Miocene evaporites. The velocity in the underlying Upper Miocene – Lower Pliocene (Mi – Pli) sediments, is 4 km/s. The Mesozoic (Me) sequence shows a velocity of about 5.5 km/s. The deeper layers, characterized by velocities 6 – 6.5 Km/s and 7 Km/s, are attributed to the Paleozoic (Pa) sequence and the crystalline basement (Bas?) respectively (Kokinou et al., 2003).

The Hellenic Trench (46.4 Km - 55.5 Km) exhibits large water depths (about 3.4 Km) (Fig. 5). Here, the sequence of the layers is the same as in the Mediterranean Ridge. Zones with velocity reversals (2.5 – 3 Km/s) are observed in the sedimentary layers. They are possibly caused by the compressive deformation of the Mediterranean ridge to the west and the extensional tectonics of the Aegean arc to the east (Lallement et al., 1994).

In the outer Hellenic Arc, a bathymetric high (55.8 Km - 72.61 Km, Fig. 6), known as frontal bulge, is followed by an extended sedimentary basin (72.61 Km - 90 Km). The seismic section and the velocity model indicate that the thickness of Mesozoic and Paleozoic sedimentary sequences is increased. The boundary of crust – upper mantle (Moho?) is slightly dipping (Fig. 6b). High velocity zones of 4 – 4.5 Km/s (Fig. 6a) are observed in the shallow layers (72.61 Km - 90 Km).

The velocity model (Figs. 7a, 8a) for the eastern portion of ION-7 (90 Km - 178.71 Km, Figs. 7, 8) is similar to the one in the extended sedimentary basin of the outer Hellenic arc. This model gives additional evidence for the large thrusts in Triassic evaporites (Ev) observed in the stacked section (95 Km - 125 Km, Fig. 7b). The Mesozoic carbonates of Paxos zone (Px) (95 Km - 135 Km) show impressive thickness (time length 2.5 s TWT). The maximum velocity is about 7 Km/s and reflections from the Moho discontinuity are not detected. A layer (4 – 4.5 Km/s, fig 8a) beneath the Upper Miocene – Lower Pliocene sediments, from 145.5 Km to 164 Km, is possibly attributed to Middle (?) Miocene (Mid?) sediments.

## SURFACE CONSISTENT DECONVOLUTION

Surface consistent deconvolution was applied after stacking on a portion of the data in order to test its effectiveness in increasing the signal to noise ratio. Surface consistent deconvolution (Levin, 1989) is a multi-channel deconvolution which generalizes the conventional trace - by - trace prediction - error filtering. Multi-channel deconvolution designs a single filter for a gather of traces. It is based on the concept that a seismic trace can be analyzed into its source, receiver, offset and CDP components. Shot and offset terms were used in the present application of surface consistent deconvolution. The deconvolution operator length was 500 ms and the “white noise” level 0.1.

The surface consistent deconvolution was applied to a selected portion of the

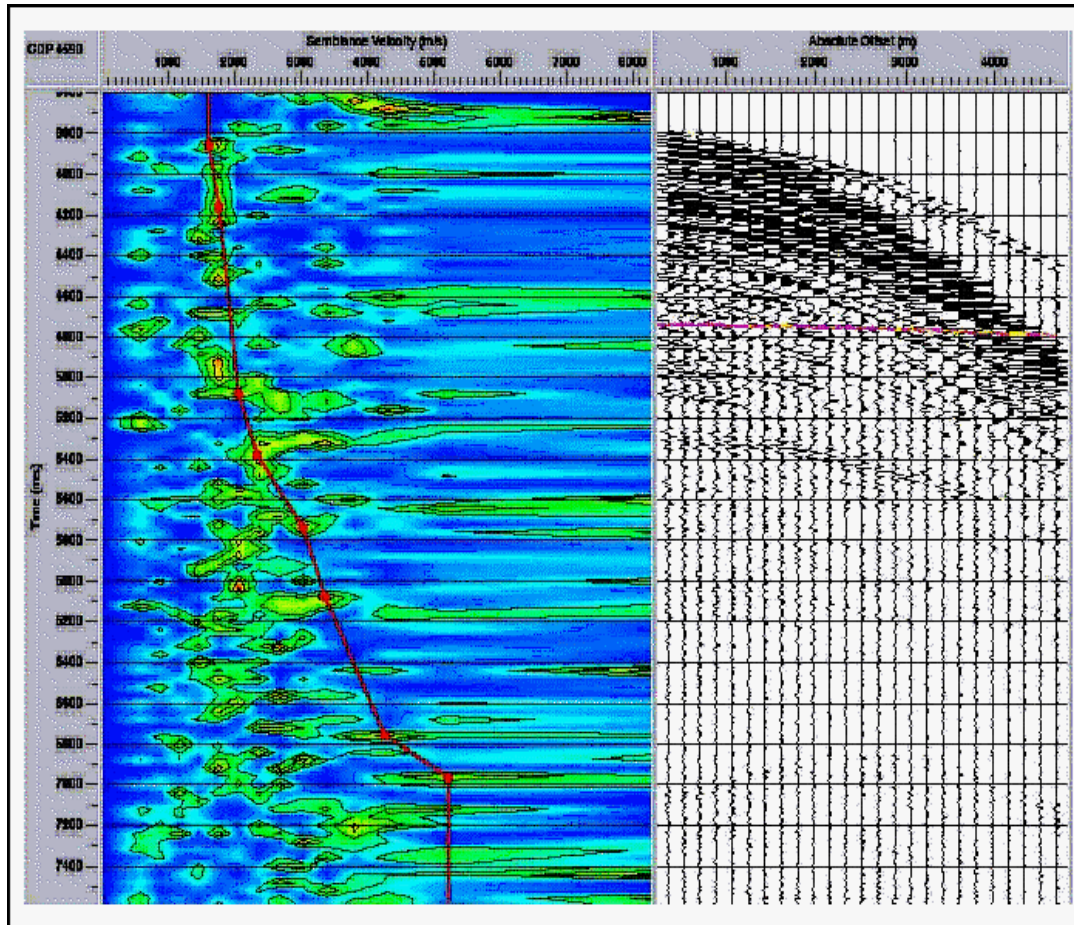


**FIG. 3:** Semblance velocity diagram for the CDP gather 4590.

stacked section located between 122.5 – 144.5 Km (Fig. 9) of the seismic line ION which images Mouna strike – slip fault with a positive flower structure (Kamberis et al., 1996) and Kefallinia diapir in Paxos zone to the west and Ionian zone to the east. The signal to noise ratio at times greater than 2.5 s TWT is low. Additionally, lateral reflections are present between 132 and 140 Km at times greater than 3 s TWT.

Figure 10 displays the stacked section after the application of the surface consistent deconvolution. The quality of the stacked section increases especially at times greater than 2.5 s TWT. Two SW dipping reflectors (at 2 – 4 s TWT and at 4.2 – 5.2 s TWT respectively) are present between 122 and 140 Km, while a third one almost flat (5.8 – 6.2 s TWT) is detected between 120 and 132 Km. The interpreted stacked section (Fig. 11) images a portion of the Hellenic arc

consisting mainly of the Pre – Apulian (Paxos) zone and partly of the Ionian zone. The Mouna Fault contractional structure and Kefallinia Diapir influence the Plio – Quaternary (P – Q) underlain by the Upper Miocene – Lower Pliocene (Mis – Pli) sediments according to geologic evidence from Kefallinia and Zakynthos islands (Underhill, 1989). The Plio – Quaternary sediments in Kefallinia Diapir are distorted by diapiric movements of Triassic evaporites (Ev). The occurrence of diapirs in hanging – wall anticlines of pre – existing thrusts has been also reported by other researchers (Kamberis et al., 1996). East and west of the Kefallinia diapir (located at 140 – 141.5 Km and 143 – 144.8 Km) neogene (Neo?) sediments at larger depths (to 2 s TWT, Fig. 11) are present.

The increased thickness of the Alpine sediments is due to the presence of the Triassic evaporites (Ev) and the

Pleistocene compressive tectonics in the Pre – Apulian zone. The Mesozoic carbonates (Px) of Paxos show an impressive thickness (time length 2 s TWT). The Ionian (Io) eastern boundary is

possibly detected under the Mouna anticline. East of the Mouna fault, the Crystalline Basement (Bas) and the Paleozoic (Pa), bend upwards.

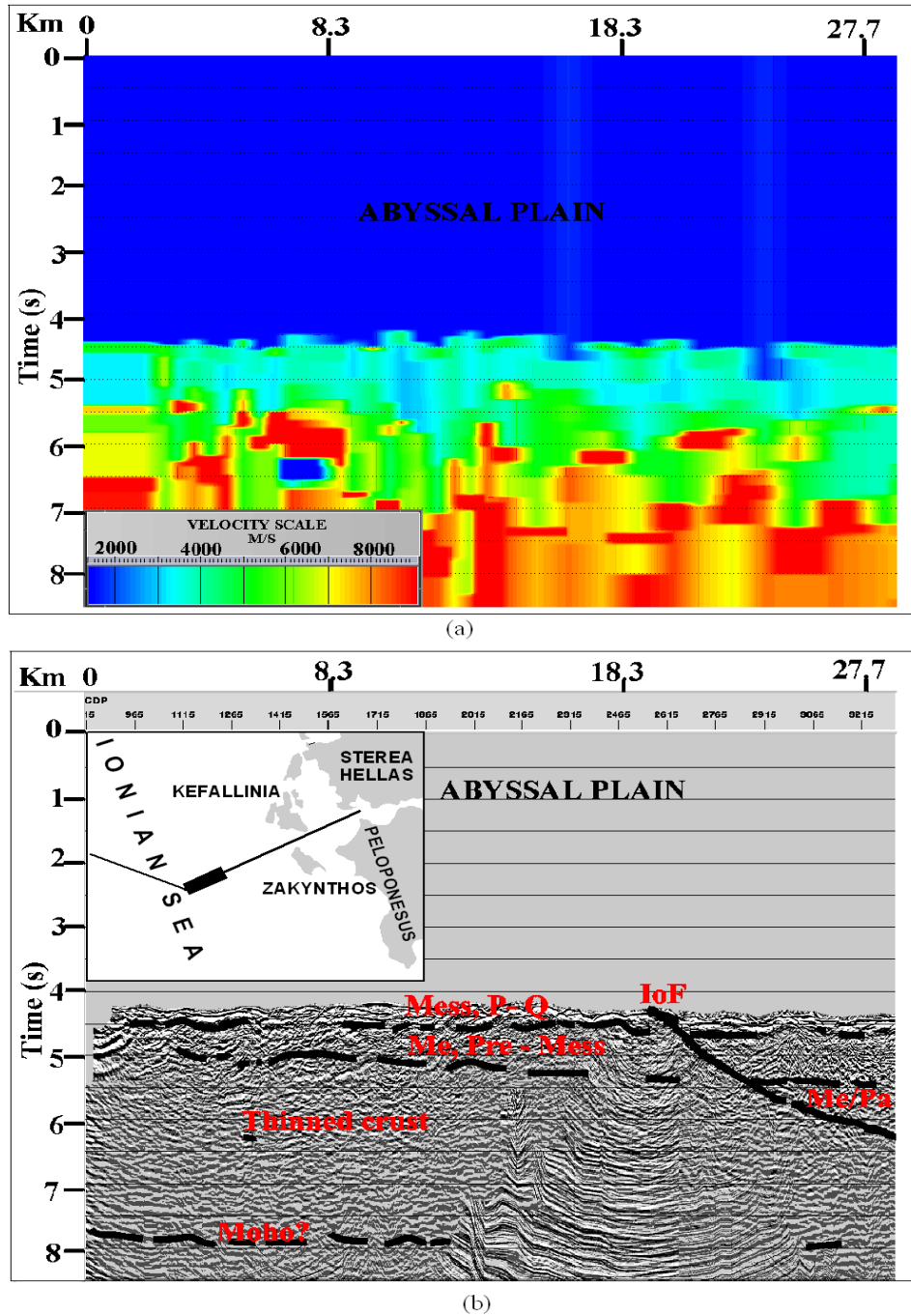
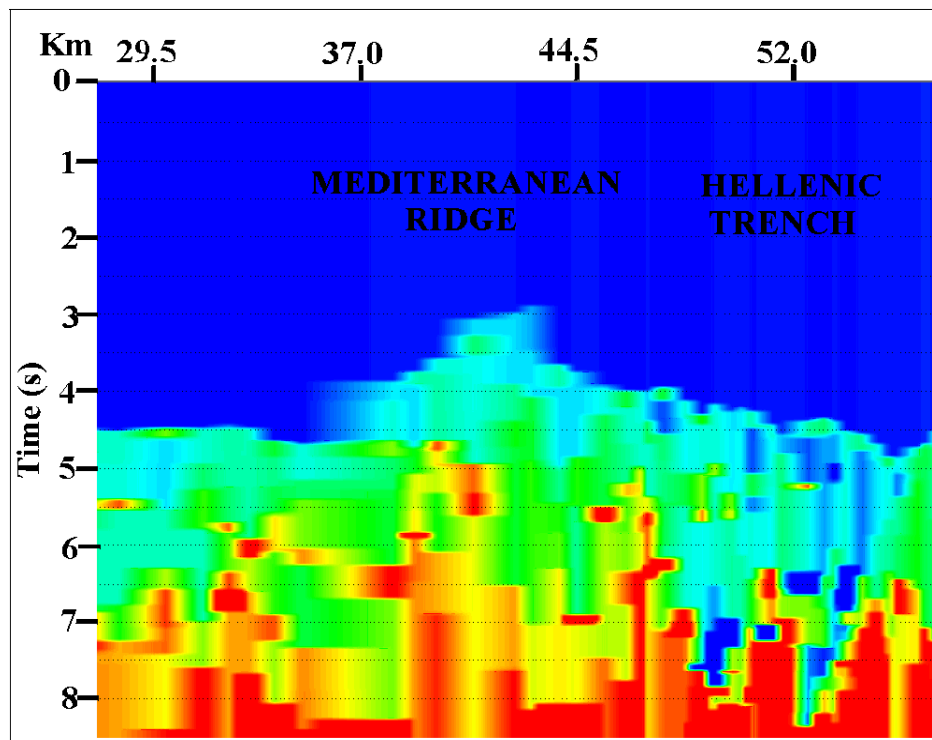
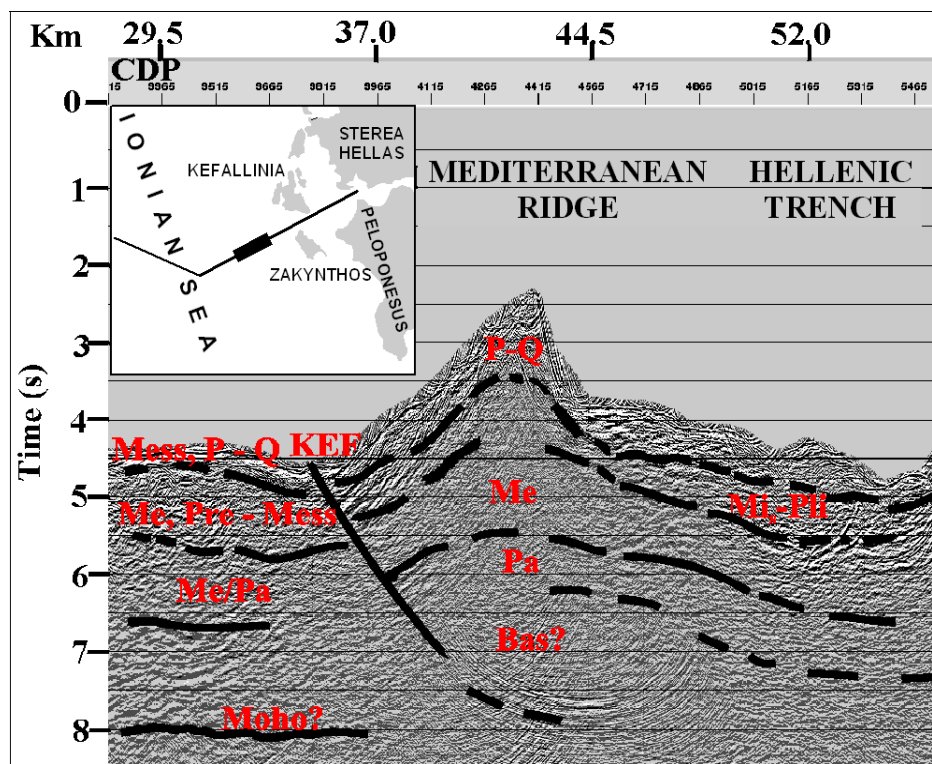


**FIG. 4:** (a) Interval velocity distribution of the section located between 0 – 28 Km (v.e = 1:1). The velocity ranges between 1.5 – 9 Km/s. (b) Interpretation of the migrated section located between 0 – 28 Km (v.e = 1:1). Mess, P – Q : Messinian, Pliocene – Quaternary sediments, Me, Pre – Mess: Mesozoic, Pre – Messinian sediments, IoF: subduction fault.

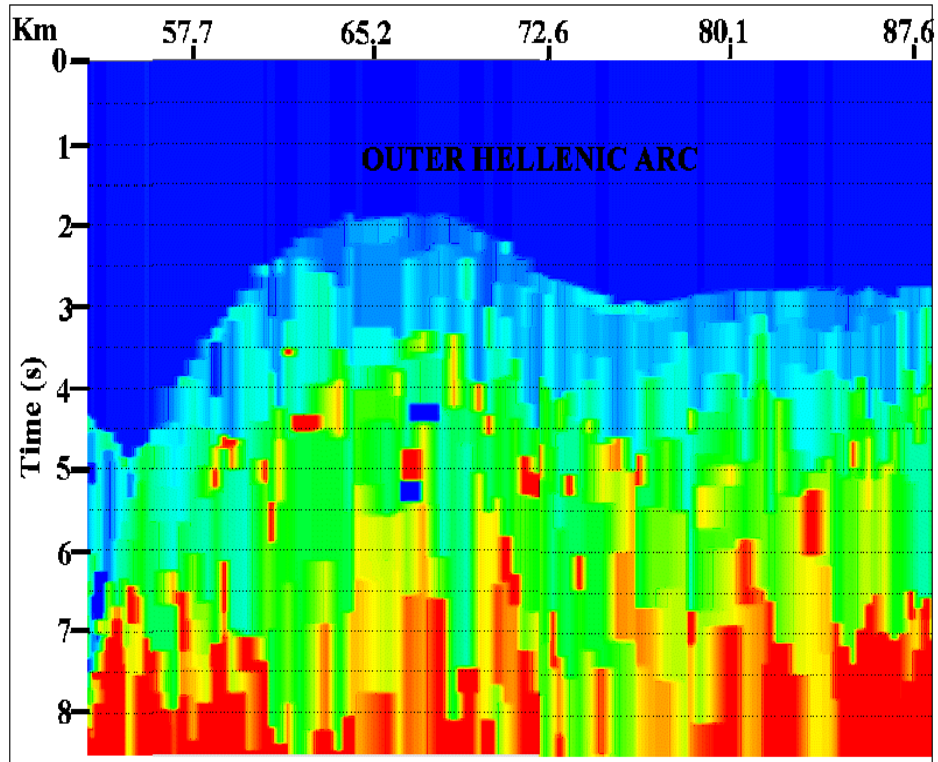


(a)

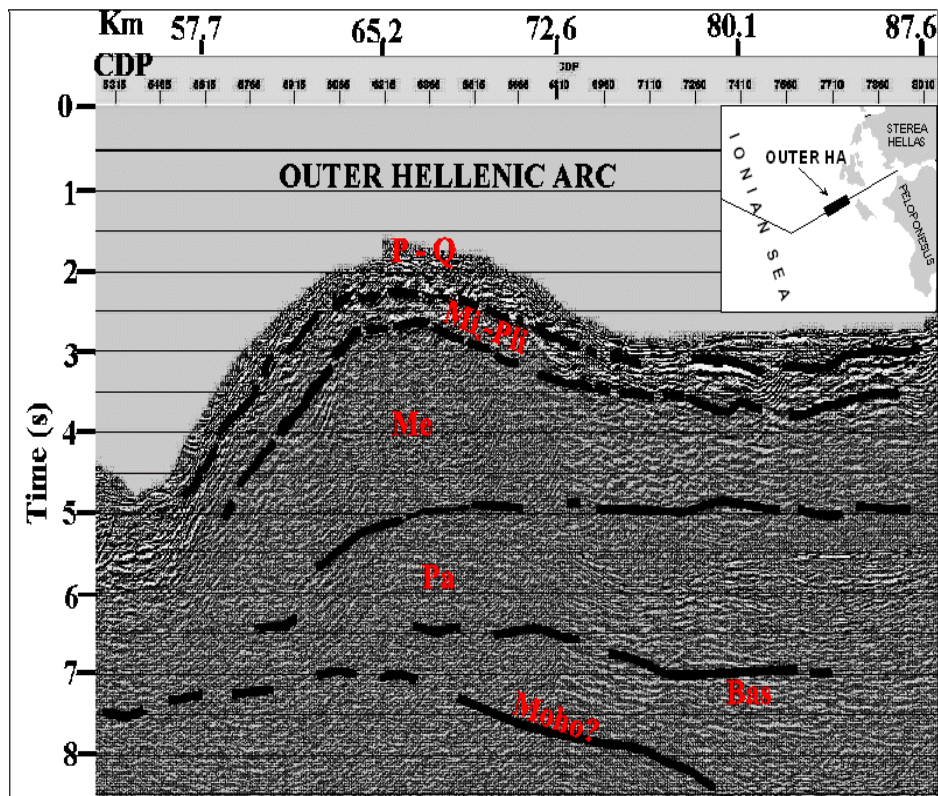


(b)

**FIG. 5:** (a) Interval velocity distribution of the section located between 28 – 55.5 Km (v.e = 1:1). The velocity ranges between 1.5 – 9 Km/s. (b) Interpretation of the migrated section located between 28 – 55.5 Km (v.e = 1:1). P – Q: Pliocene – Quaternary sediments, Mi – Pli: Upper Miocene – Lower Pliocene sediments, Me: Mesozoic sequence, Pa: Paleozoic sequence, Bas?: basement, KEF: Kefallina transform fault.

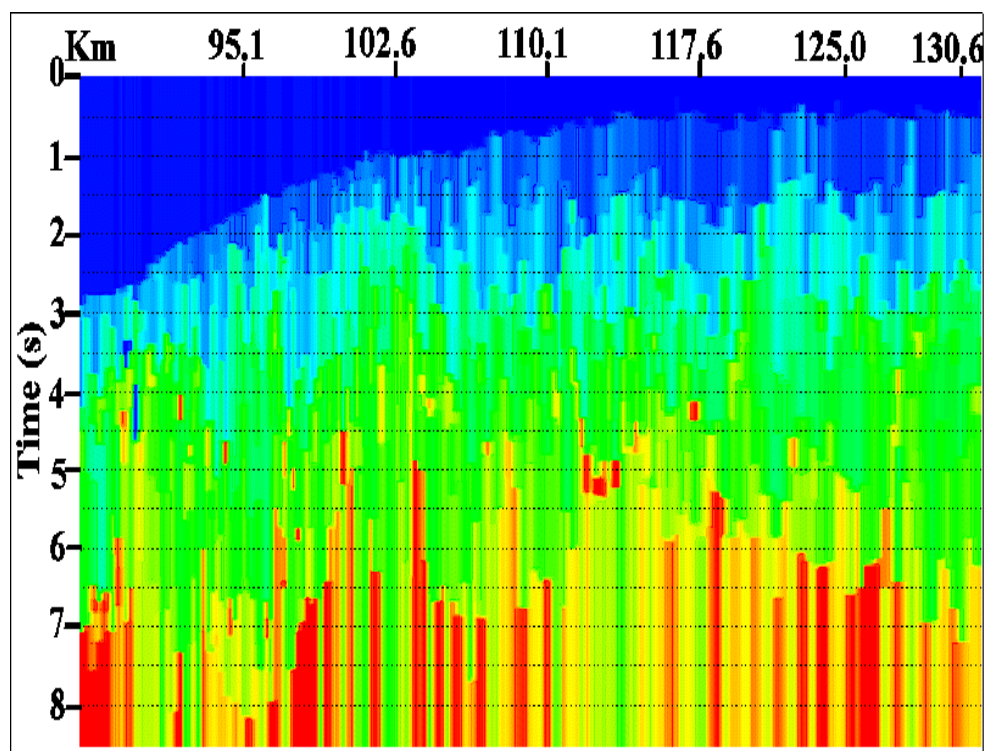


(a)

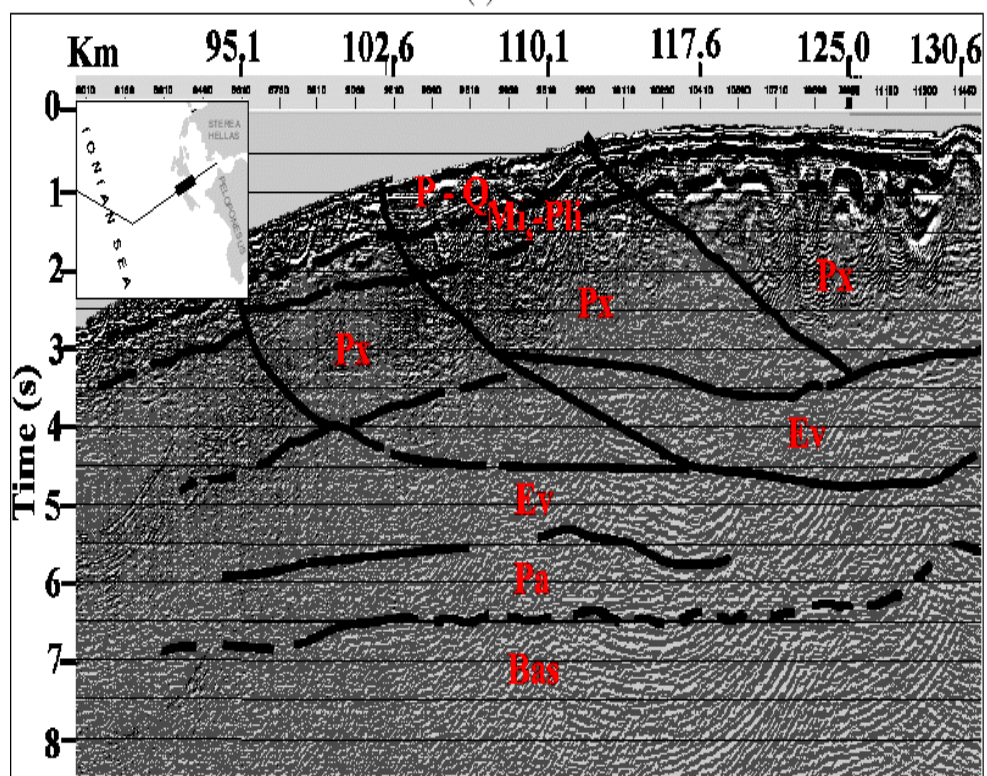


(b)

**FIG. 6:** (a) Interval velocity distribution of the section located between 53 – 88 Km (v.e = 1:1). The velocity ranges between 1.5 – 9 Km/s. (b) Interpretation of the migrated section located between 53 – 88 Km (v.e = 1:1).



(a)



(b)

**FIG. 7:** (a) Interval velocity distribution of the section located between 88 – 131 Km (v.e = 1:1). The velocity ranges between 1.5 – 9 Km/s. (b) Interpretation of the migrated section located between 88 - 131 Km (v.e = 1:1). Px: Mesozoic carbonate of Paxos zone, Ev: Triassic evaporites.

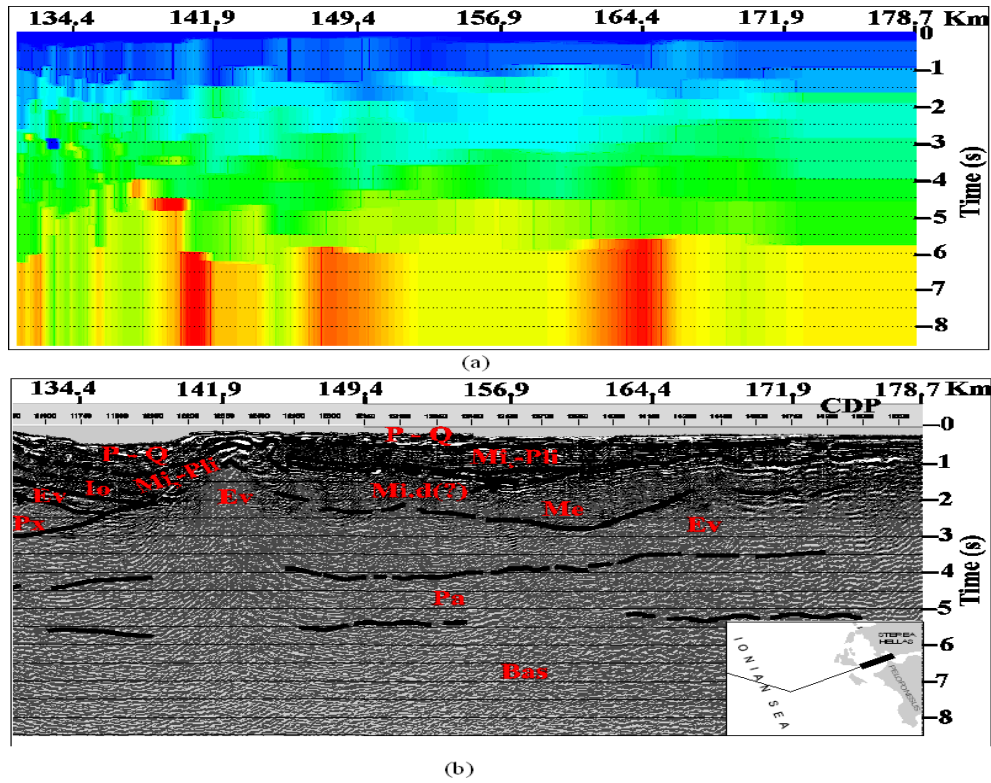


FIG. 8: (a) Interval velocity distribution of the section located between 131 – 178. 71 Km (v.e = 1:1). The velocity ranges between 1.5 – 9 Km/s. (b) Interpretation of the migrated section located between 131 – 178.71 Km (v.e = 1:1). Mi.d(?): Middle (?) Miocene sediments, Io: Mesozoic carbonates of Ionian zone.

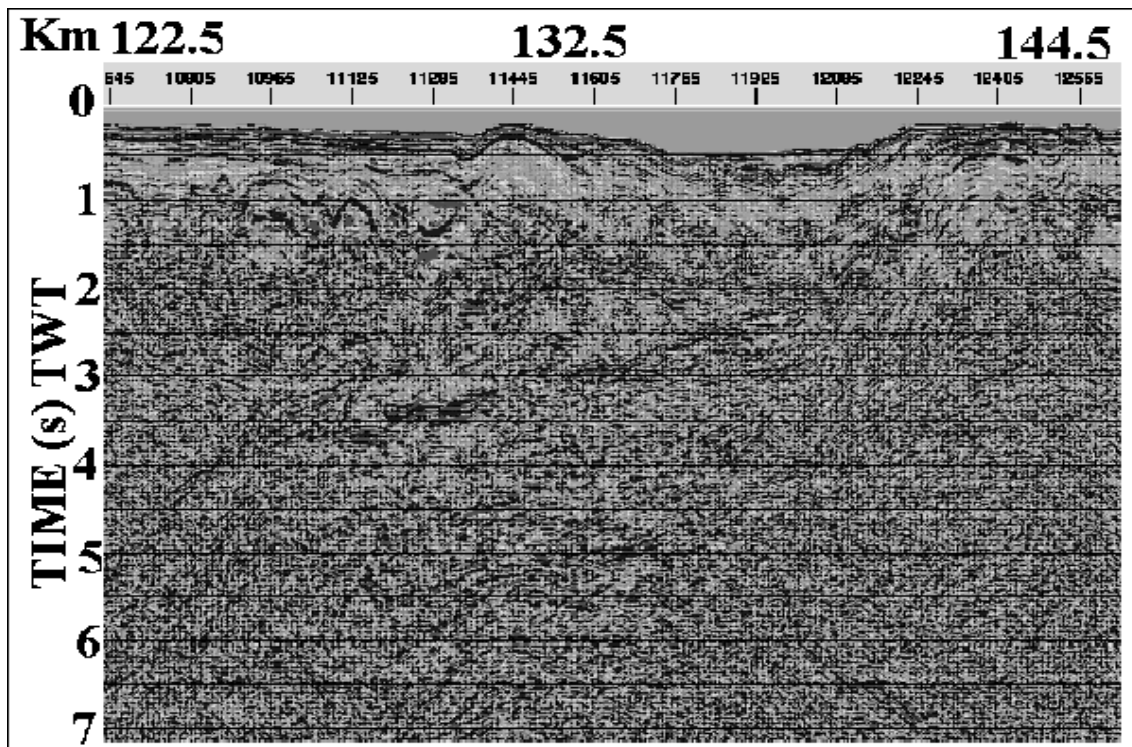
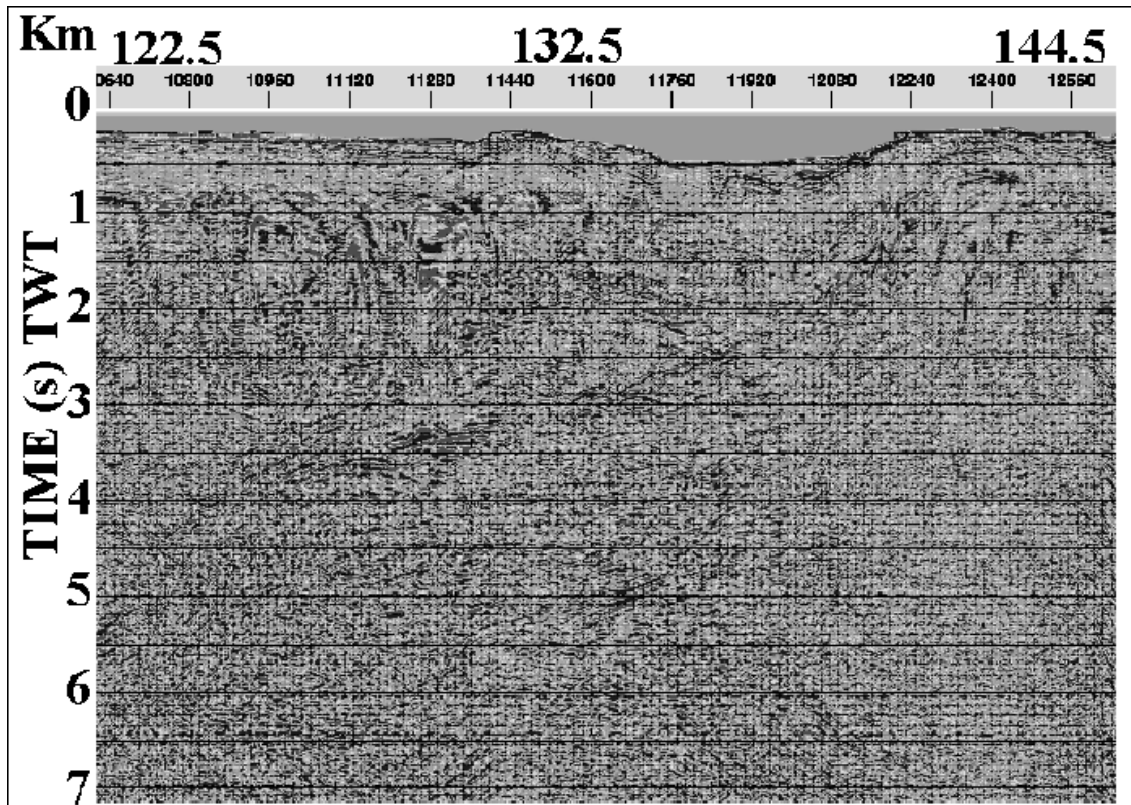


FIG. 9: Stacked section (v.e = 1:1) located between 122.5 – 144. 5 Km of the seismic line ION – 7 before the application of the surface consistent deconvolution



**FIG. 10:** Stacked section ( $v.e = 1:1$ ) located between 122.5 – 144.5 Km after the application of the surface consistent deconvolution.

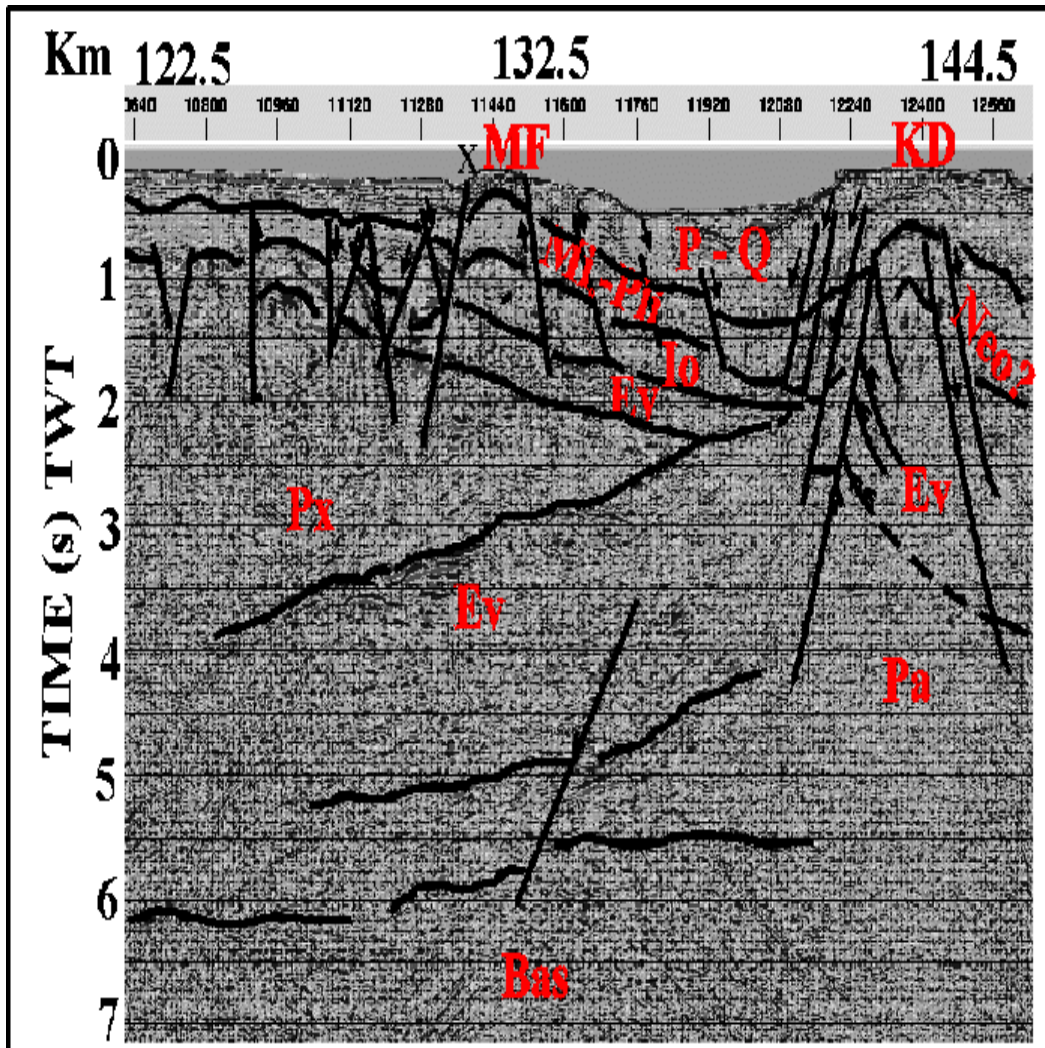
### POSTSTACK KIRCHHOFF MIGRATION - INSTANTANEOUS ATTRIBUTES

Kirchhoff migration was chosen since it offers relative speed and good handling of the vertically variant velocity fields and steep dips. Migration involves repositioning data elements to make their locations appropriate to the locations of the associated reflectors or diffracting points. Kirchhoff migration (Hagedoorn, 1954) is also known as the diffraction summation method. The migration scheme based on summation method consists of searching the input data in  $(x, t)$  space for energy that would have resulted if a diffracting source (Huygens' secondary source) were located at a particular point in the output  $(x, z)$  space. This search is carried out by summing the amplitudes in  $(x, t)$  space along the diffraction curve that corresponds to Huygens' secondary source at each point in the  $(x, z)$  space (Yilmaz, 1987).

The migration aperture was computed from the data, the maximum dip was 60 ms / trace and the maximum frequency to migrate was 60 Hz. RMS velocities were reduced by 20% in order to avoid overmigration.

The major instantaneous attributes, are the instantaneous frequency, instantaneous amplitude and instantaneous phase (Taner, 1978). Hilbert transform is a conventional method for instantaneous parameter estimation.

The instantaneous attributes were computed for a portion of the migrated section. Figure 12 presents the reflection strength for a selected portion of the migrated section, located between 122.5 – 144.5 Km. The main events are indicated by the symbols a, b, c and d. In comparison with the interpreted stacked section (Fig. 11) event a corresponds to the bottom of Ionian evaporites, event b to the bottom of Mesozoic carbonates of Paxos zone, event c to the top of Paleozoic and event c to the top of basement respectively.



LEGEND

- P-Q:** Pliocene - Quaternary
- Neo?:** Neogene
- Mi-Pl:** Upper Miocene - Lower Pliocene
- Ev:** Triassic evaporites
- Px:** Carbonate of Pre - Apulia zone (Paxos)
- Io:** Carbonate of Ionian zone
- Pa:** Paleozoic
- Bas:** Crystalline Basement
- MF:** Mounta Fault
- KD:** Kefalinia Diapir
- Seismic reflector
- - -** Possible seismic reflector



- Reverse Fault
- Normal Fault
- Strike slip fault

FIG. 11: Interpreted stacked section (v.e = 1:1) located between 122.5 – 144.5 Km after the application of the surface consistent deconvolution

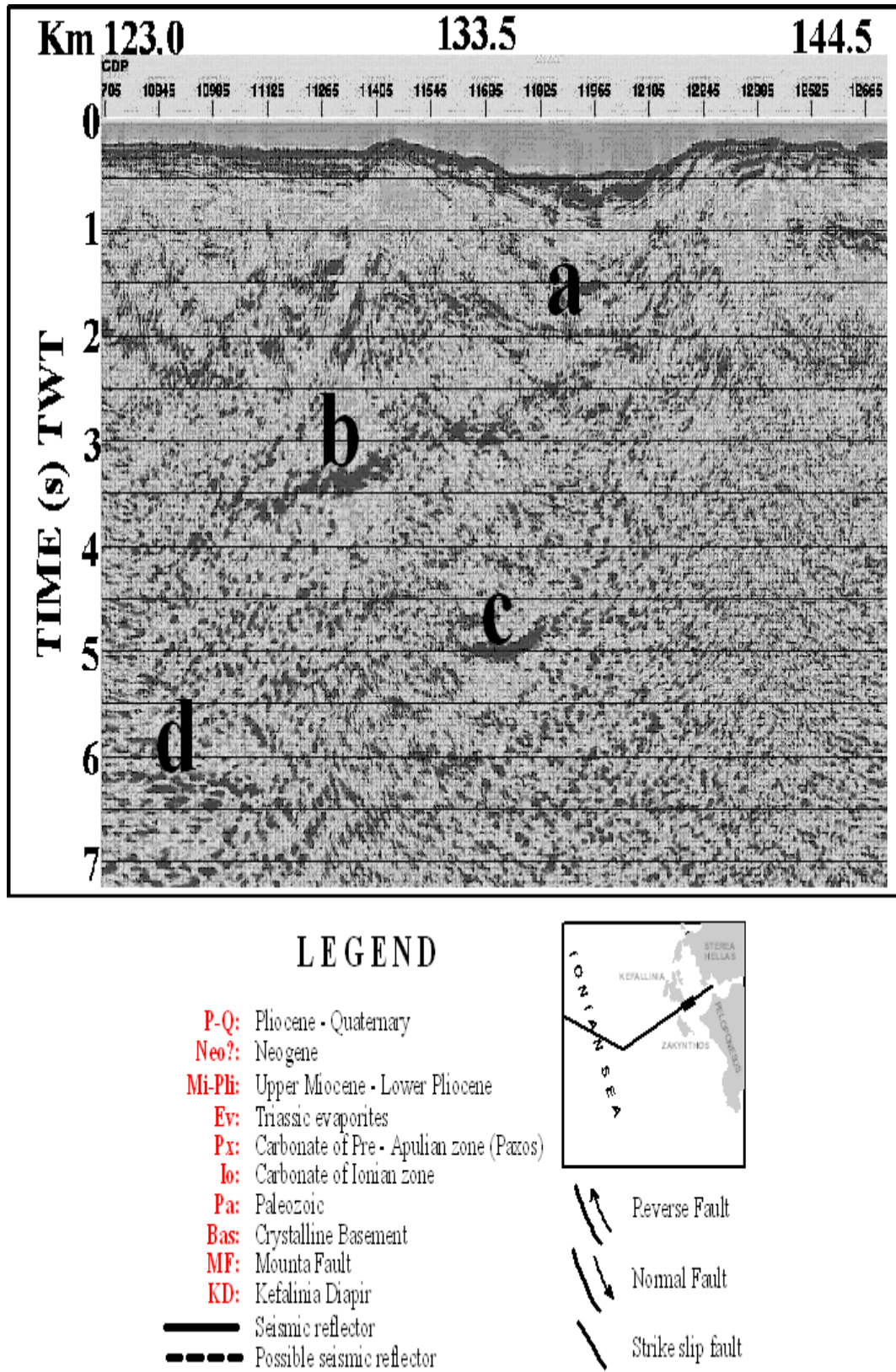


**FIG. 12:** Computation of the reflection strength for the migrated section (v.e = 1:1) located between 122.5 – 144.5 Km.

## CONCLUSIONS

In this study, seismic processing including demultiple methods, surface consistent deconvolution, Kirchoff migration and attribute analysis is applied to reflection data along the seismic line ION-7. Images of the subsurface are generated for the western margin of the Hellenic Arc.

Surface consistent deconvolution was proved helpful in increasing the signal to noise ration and reducing the effect of lateral reflections. The quality of the stacked section was increased especially at great times and helped estimating the deeper horizons. Attribute analysis was applied on the migrated section and helped estimating the high reflectivity horizons.

A complicated velocity model for the area of study was derived by the velocity analysis. High velocities attributed to Messinian evaporates characterize the shallow layers in the western portion of ION-7 compared to the ones in eastern portion. The velocity model indicates that the crust of the Ionian abyssal plain appears extremely thin (12 – 15 Km). Velocity reversals are observed in the Hellenic Trench caused by the compressive deformation of the Mediterranean ridge and the extensional tectonics of the Aegean arc. In the Pre-Apulian zone the velocity model indicates that the thickness of the evaporites and carbonates increases.

## ACKNOWLEDGMENTS

The authors are deeply indebted to HELLENIC PETROLEUM Company (EL.PE) and the University of Athens for the availability of the data. Special thanks are due to the editors and reviewers for the suggestion of the constructive changes in this paper.

## REFERENCES

- Barazanghi, M., & Brown, L., 1986, Reflection Seismology: A Global Review, and Reflection Seismology: The Continental Crust, Geodynamics Series, **13 & 14**, American Geophysical Union, Washington DC.
- Clowes, R.M., Calvert, A.J., Eaton, D.W., Hajnal, Z., Hall, J., Ross, G.M., 1996, LITHOPROBE reflection studies of Archean and Proterozoic crust in Canada: Tectonophysics **264**, 65 –88.
- Damotte, B., Fuchs, K., Lueschen, E., Wenzel, F., Schlich, R., and Toreilles, G., 1987, Wide angle Vibroseis test across the Rhyne graben: Geophys. J.R. Astron. Soc., **89**, 313 – 318.
- Dercourt, J., Zonenshain, L.P., Ricon, L.E., Kazmin, V.G., Le Pichon, X., Knipper, A.L., Grandjaquet, C., Sbertshikov, I.M., Geysant, J., Lepvrier, C., Pechersky, D.H, Boulin, J., Sibuet, J.C., Savostin, L.A., Sorokhtin, O., Westphal, M., Bazhenov, M.L., Lauer, J.P., Biju – Duval, B., 1986, Geological evolution of the Tethys belt from the Atlantic to the Pamirs since the Lias: Tectonophysics, **123**, 241 – 315.
- Finetti, I., and Morelli, C, 1973, Geophysical exploration of the Mediterranean Sea: Boll. Geofis. Teor. Appl., XV (**60**), 261 –341, 14 maps, Trieste, Udine.
- Finetti, I., 1982, Structure stratigraphy and evolution of the central Mediterranean Sea: Bolletino di Geofisica Teorica et Applicata, **15**, 263 – 341.
- Giese, P., and Morelli, C., 1973, La struttura della crosta terrestre in Italia, in: Atti Convegno sul Tema: Moderne Vedute sulla Geologia dell' Apennino, Rome, 16 –18, February, 1972.
- Griffiths, L. J., Smolka, F. R., and Trembly, L. D., 1978, Adaptive deconvolution: a new technique for processing time varying seismic data: Reprinted from Geophysics, **42**, 4, 742-759.
- Hagedoorn, J. G., 1954, A process of seismic reflection interpretation: Geophysical Prospecting, **2**, 85 – 127.
- Hirn, A., Sachpazi, M., Siliqi, R., McBride, J., Marnelis, F., Cernobori, L., and STREAMERS – PROFILES group, 1996, A traverse of the Ionian Islands front with coincident normal incidence/ and wide angle seismics: Tectonophysics, **264**, 35 –49.
- IGME, Seismotectonic map, 1:500,000.
- Kamberis, E., Marnelis, F., Loucoyannakis, M., Maltezu, F., Hirn,

- A., and STREAMERS group, 1996, Structure and deformation of the External Hellenides based on seismic data from offshore Western Greece: EAGE Special Publication, **5**, 207 – 214.
- Klemperer, S.L., Brown, L., Oliver, J.E., Ando, C.J., Czuchra, B.L., Kaufman, S., 1985, Some Results of COCORP seismic reflection profiling in the Grenville – age Adirondack Mountains New York State: *Can. J. Earth Sci.*, **22**, 141 – 153.
- Kokinou E., Vafidis A., 2002, Deep – water multiple suppression on prestack and poststack reflection data from Ionian Sea: submitted to *Geophysical Prospecting*.
- Kokinou, E., Kamberis, E., Vafidis, A., Hirn, A., and Monopolis, D., 2003, Crustal model of Ionian Sea based on deep seismic reflection data from offshore Western Greece: submitted to *Marine Geology*.
- KTB – Research Group Black Forest, 1987, Pre – drilling reflection survey of the Black Forest, SW Germany: *Geophys. J.R. Astron. Soc.*, **89**, 325 – 332.
- Lallement, S., Truffert, C., Jolivet, L., Henry, P., Chamot – Rooke, N., De Voogd, B., 1994, Spatial Transition from Compression to Extension in the Western Mediterranean Ridge Accretionary Complex: *Tectonophysics*, **234**, 33 – 52.
- Levin, S.A., 1989, Surface – consistent deconvolution: *Geophysics*, **54**, No. 9, 1123 – 1133.
- Makris, J., Nicolich, R., Weigel, W., 1986, A seismic Study in the Western Ionian Sea: *Annales Geophysical*, **4**, B 6, 665 – 678.
- Makris, J., 1975, Crustal Structure of the Aegean Sea and the Hellenides obtained from Geophysical Surveys: *Rapp. Comm. Int. Mer. Médit.*, **23**, 4a, 201 – 202, 1 fig.
- Matthews, D., and Smith, C., 1987, Deep seismic reflection profiling of the continental lithosphere: *Geophys. J. R. astr. soc.*, **89**, vii – xii.
- Morelli, C., Gantar, C., Pisani, M., 1975, Bathymetry gravity (and magnetism) in the Strait of Sicily and in the Ionian Sea: *Boll. Geofis. Teor. Appl.*, **17**, 39 – 58.
- Moretti, I., and Royden, L. 1978, Deflection, Gravity anomalies and Tectonics of doubly subducted continental lithosphere: Adriatic and Ionian seas: *Tectonics*, **7**, 4, 875 – 893.
- Nicolich, R., Cernobori, L., Romanelli, M., Petronio, L., 1994, The Ionian Basin and its margins off southern and eastern Calabria: Draft basis of paper for Budapest Proceedings in Tectonophysics presented at EGS Grenoble, April 1994; Deep Seismics Budapest, September 1994; pre – Vienna EEC report, 1- 17.
- 2D PROMAX reference, Version 6.0.
- Taner, M.T., 1978, Complex seismic trace analysis: *Geophysics*, **44**, 1041 – 1063.
- Underhill, J.R., 1989, Late Cenozoic deformation of the Hellenide foreland, western Greece: *Geological Society of America Bulletin*, **101**, 613 – 634.
- Vejmelek, L., and Tomek, C., 1989, Deep reflection seismic profile 598, in the southwestern part of the Transcarpathian depression: *Geophysical transactions*, **35**, 1 – 2, 65 – 76.
- Weber, F., Schmoeller, R., Fruhwirth, R.K., 1996, Results of deep reflection seismic measurement south of Rechnitz/ Burgenland/ Austria: *Geophysical transactions*, **40**, 1 – 2, 79 – 93.
- Weigel, W., 1974, Crustal Structure under the Ionian Sea: *Short Communications, J. Geophys.*, **40**, 137 – 140.
- Wiggins, J. W., 1988, Attenuation of complex water bottom multiples by wave equation – based prediction and subtraction: *Geophysics*, **53**, No. 12, 1527 – 1539.
- Yilmaz, Oz., 1987, *Seismic data analysis: Processing, Inversion and Interpretation of Seismic Data*, V. I and II: Society of Exploration Geophysicists, Tulsa.